Electronic Supplementary Material (ESI) for Journal of Materials Chemistry C.
This journal is © The Royal Society of Chemistry 2016

Self-assembled Nano rods of Bay functionalized perylenediimide: Cu^{2+} based 'turn on' response for INH, complementary NOR/OR and TRANSFER logic functions and fluorosolvatochromism

Prabhpreet Singh[a,*] Kapil Kumar[a], Gaurav Bhargava[b] and Subodh Kumar[a]

[a]*Department of Chemistry, UGC Centre for Advanced Studies, Guru Nanak Dev University, Amritsar 143 005, India*
[b]*Department of Applied Sciences, Punjab Technical University, Kapurthala-144601, Punjab, India*

Table of contents

∗ Corresponding author. Tel.: +91-8427101534.

E-mail: prabhpreet.chem@gndu.ac.in

1. Spectroscopic data of PDI-DMEA

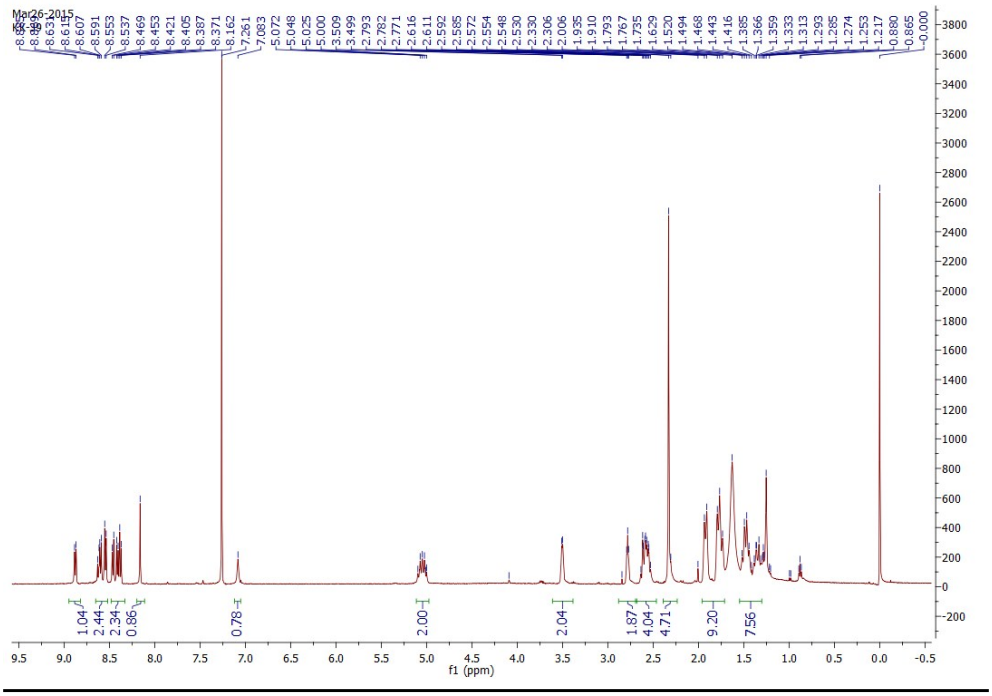

Fig S1a: ^{1}H NMR spectrum of the **PDI-DMEA**.

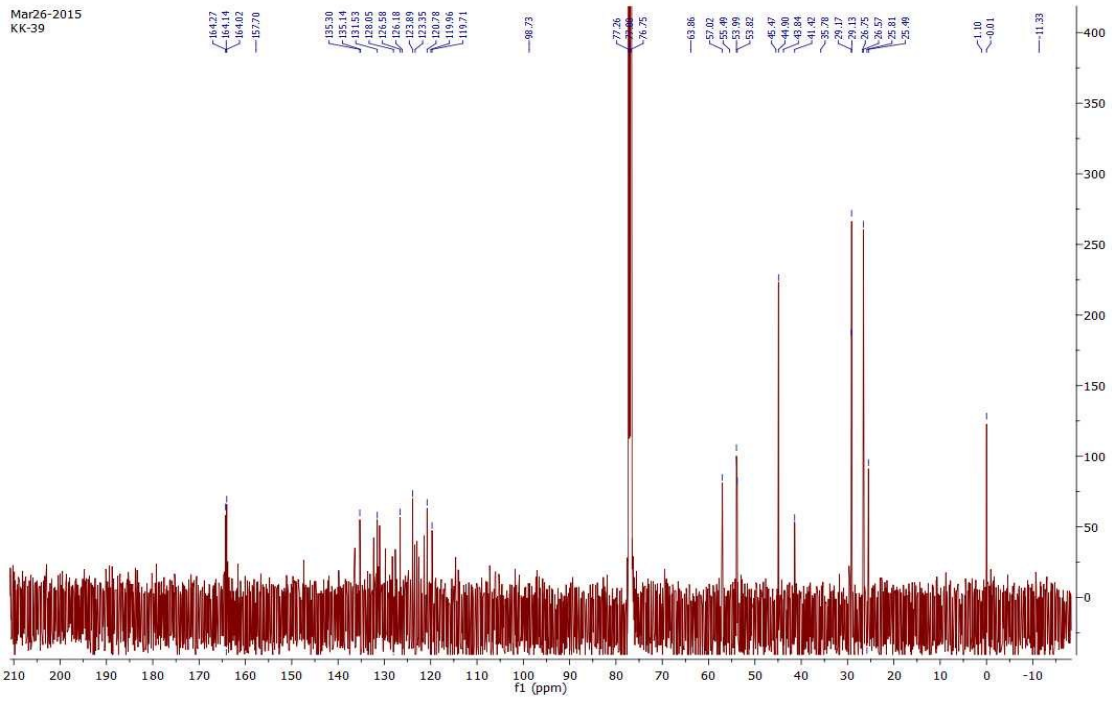

Fig S1b: ^{13}C NMR spectrum of the **PDI-DMEA**.

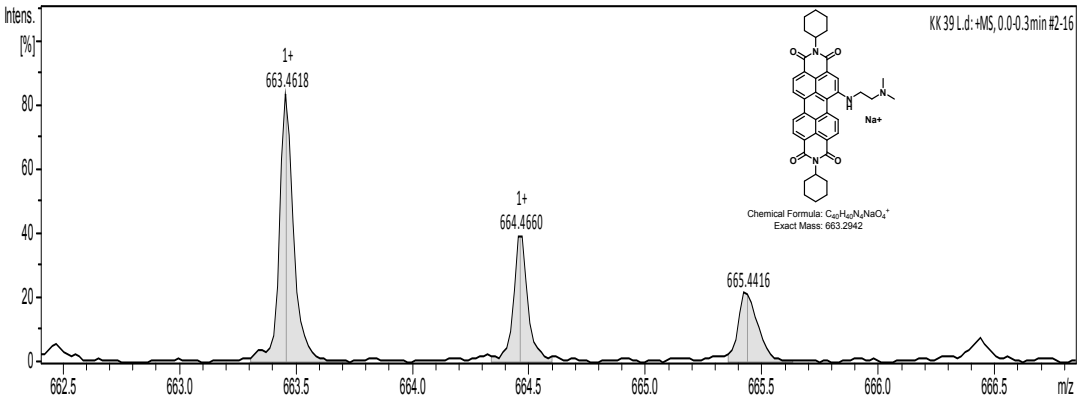

Fig S1c: Mass spectrum of the **PDI-DMEA**.

2. Wide angle X-ray diffraction of PDI-DMEA

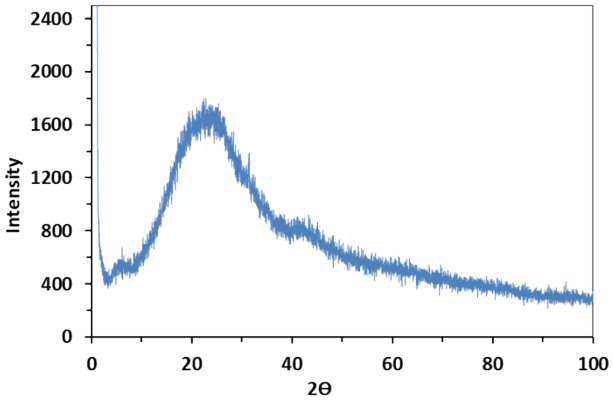

Fig. S2 WXRD data of **PDI-DMEA** showing amorphous nature of the **PDI-DMEA**.

3. Spectroscopic data of PDI-NO_2 and PDI-NH_2

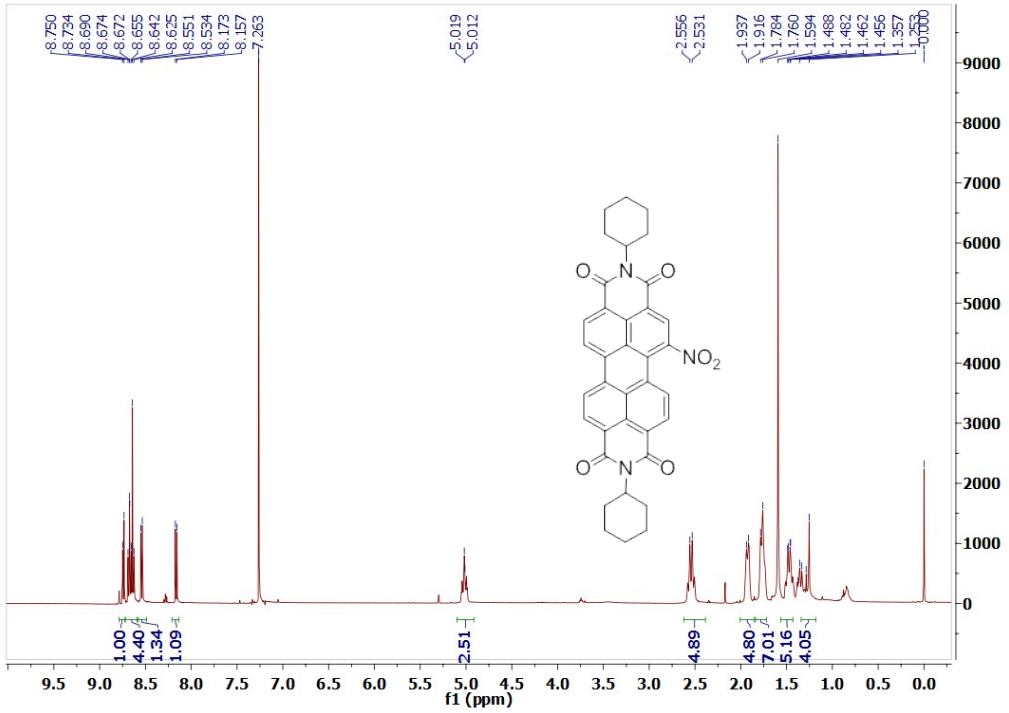

Fig S3a: ^{1}H NMR spectrum of **PDI-NO_2**.

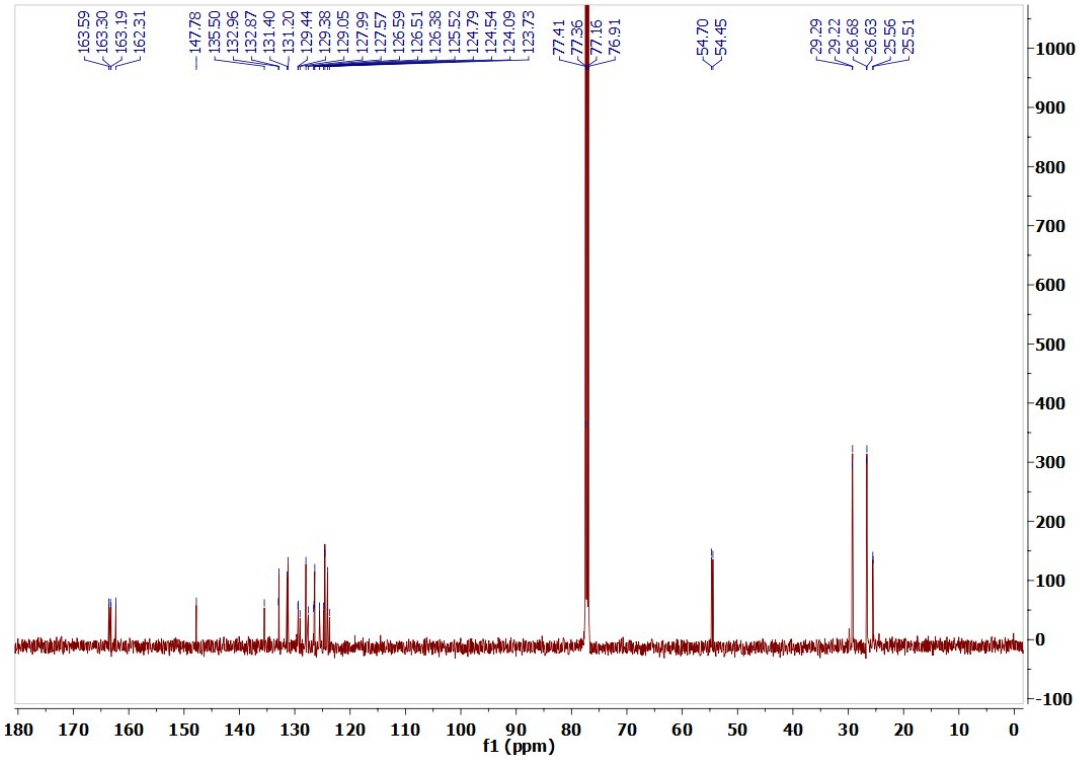

Fig. S3b ^{13}C NMR spectrum of **PDI-NO_2**.

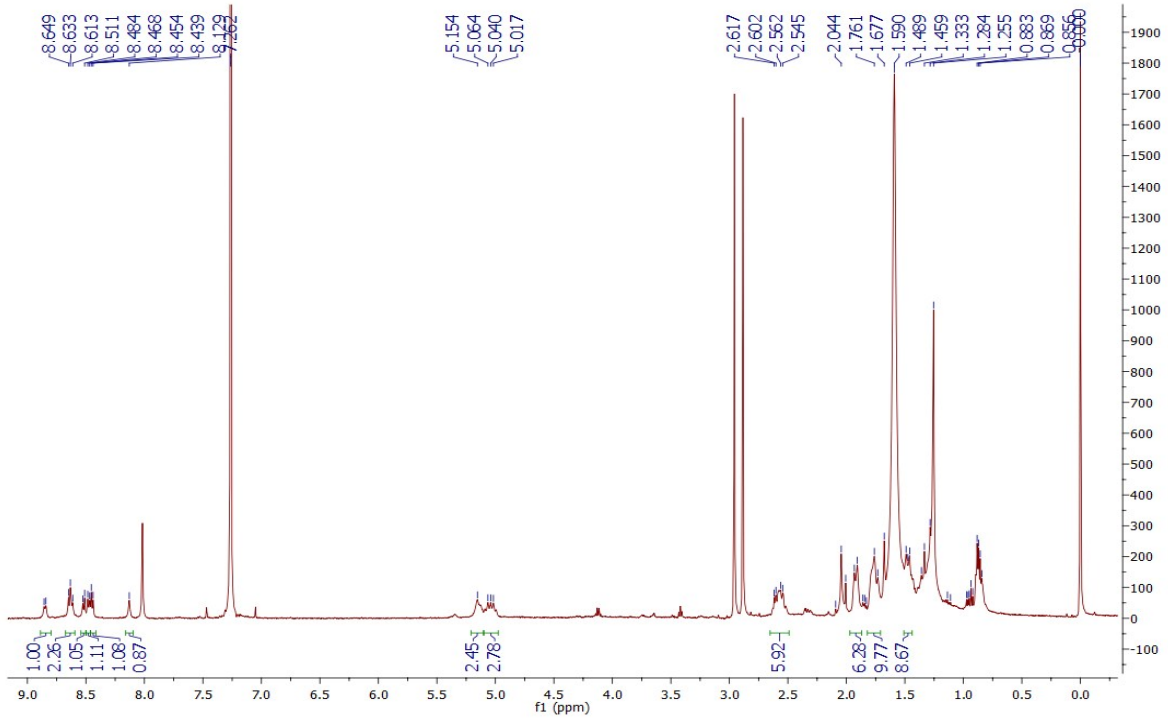

Fig S4a: ^{1}H NMR spectrum of **PDI-NH$_2$**.

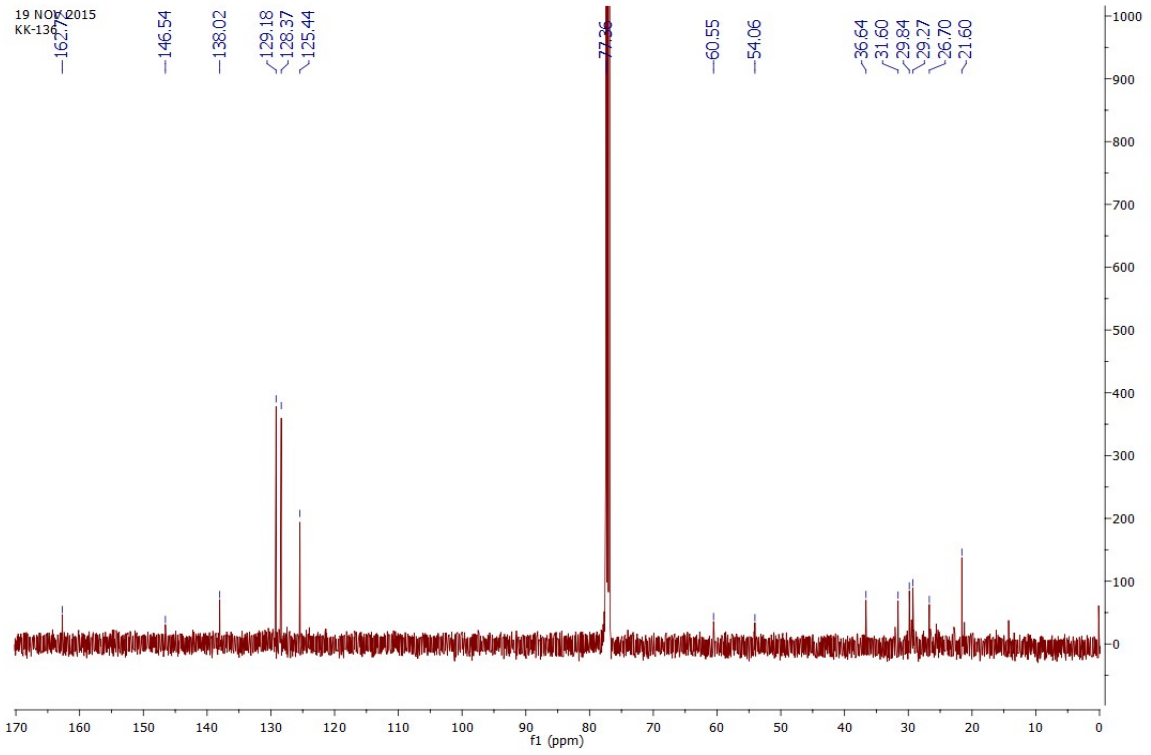

Fig. S4b ^{13}C NMR spectrum of **PDI-NH$_2$**.

4. SEM Images of PDI-DMEA

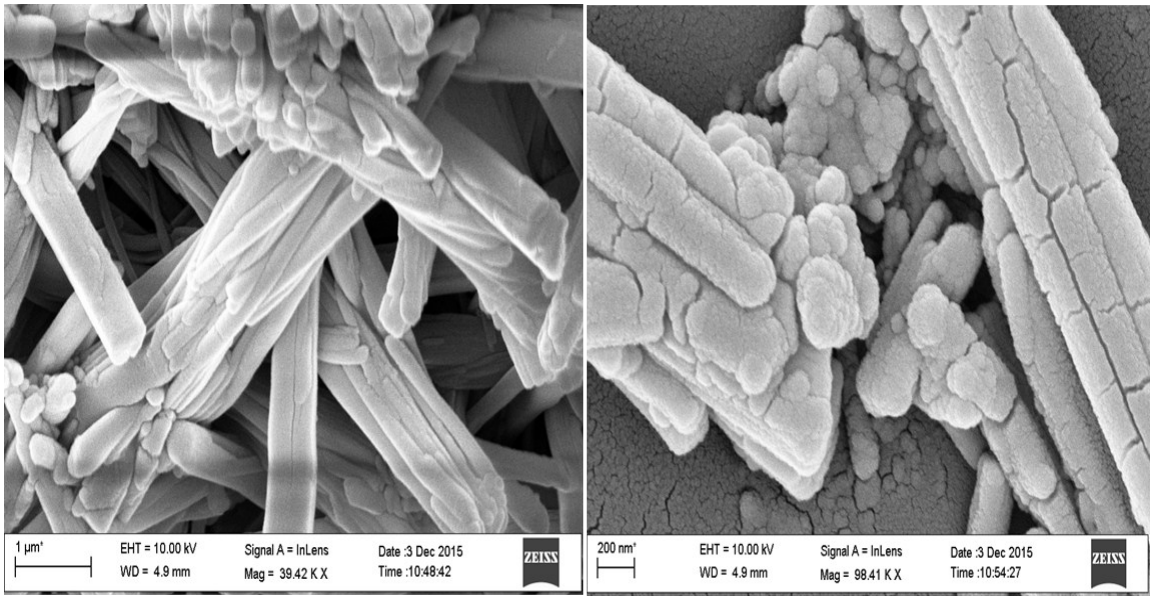

Fig. S5 Nano rods self-assembly of **PDI-DMEA** (25 µM) as observed in SEM images taken in CH_3CN solution.

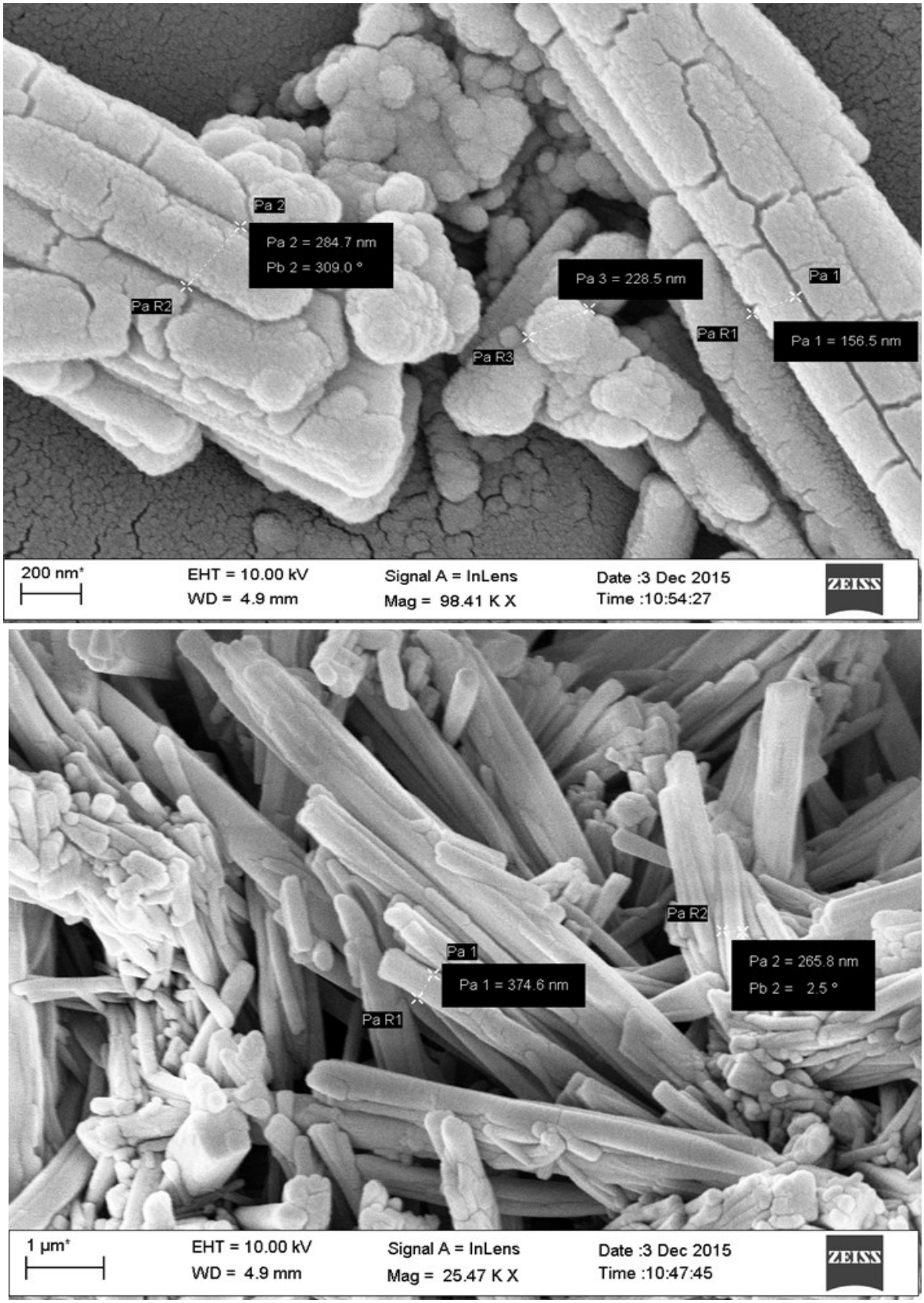

Fig. S6a Nano rods self-assembly of **PDI-DMEA** (25 µM) as observed in SEM images taken in CH_3CN solution with labeling of diameter values.

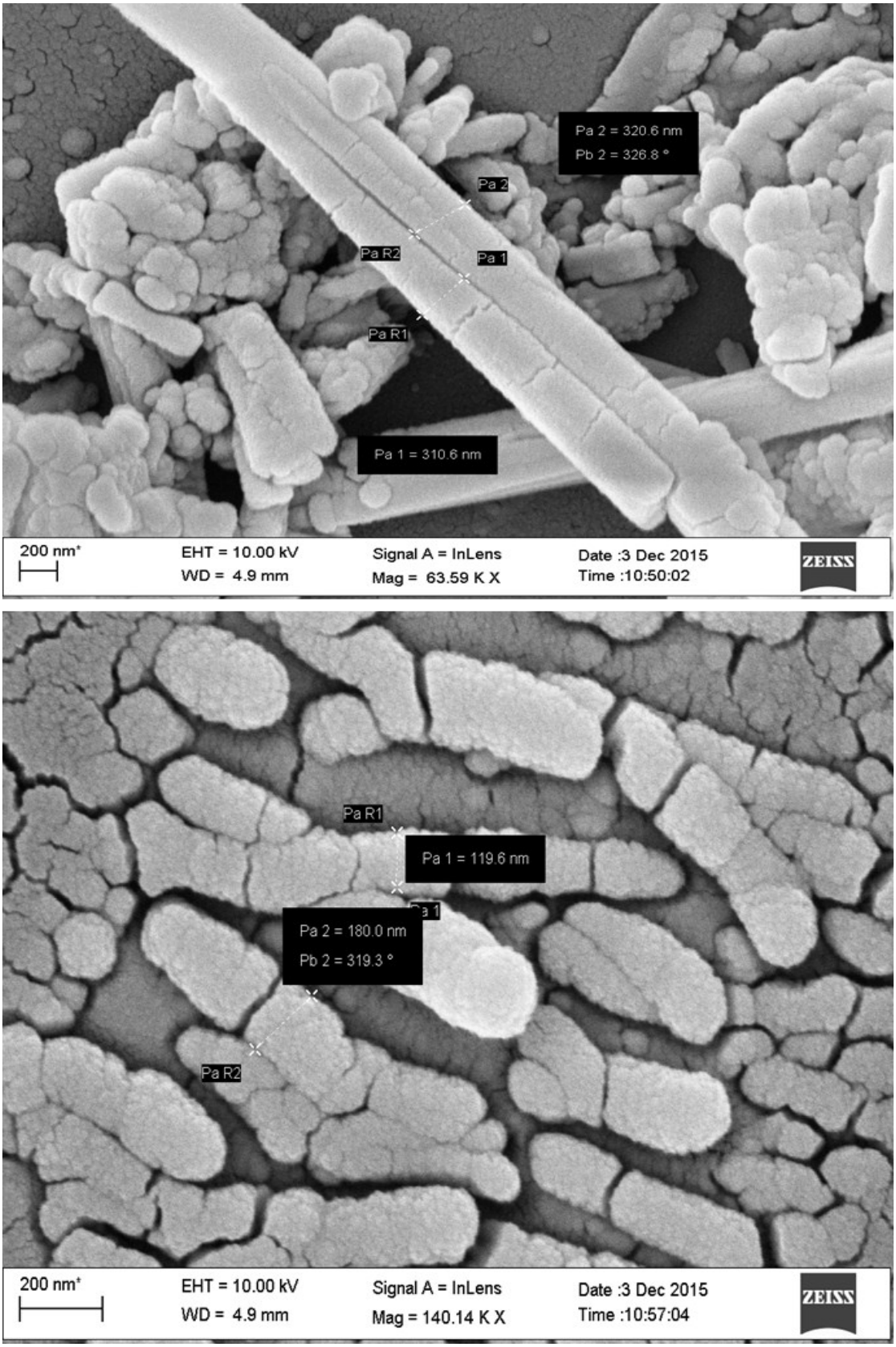

Fig. S6b Nano rods self-assembly of **PDI-DMEA** (25 μM) as observed in SEM images taken in CH_3CN solution with labeling of diameter values. Some of the spherical structures are in process of transforming into Nanorods.

5. SEM Images of PDI-DMEA+Cu^{2+}

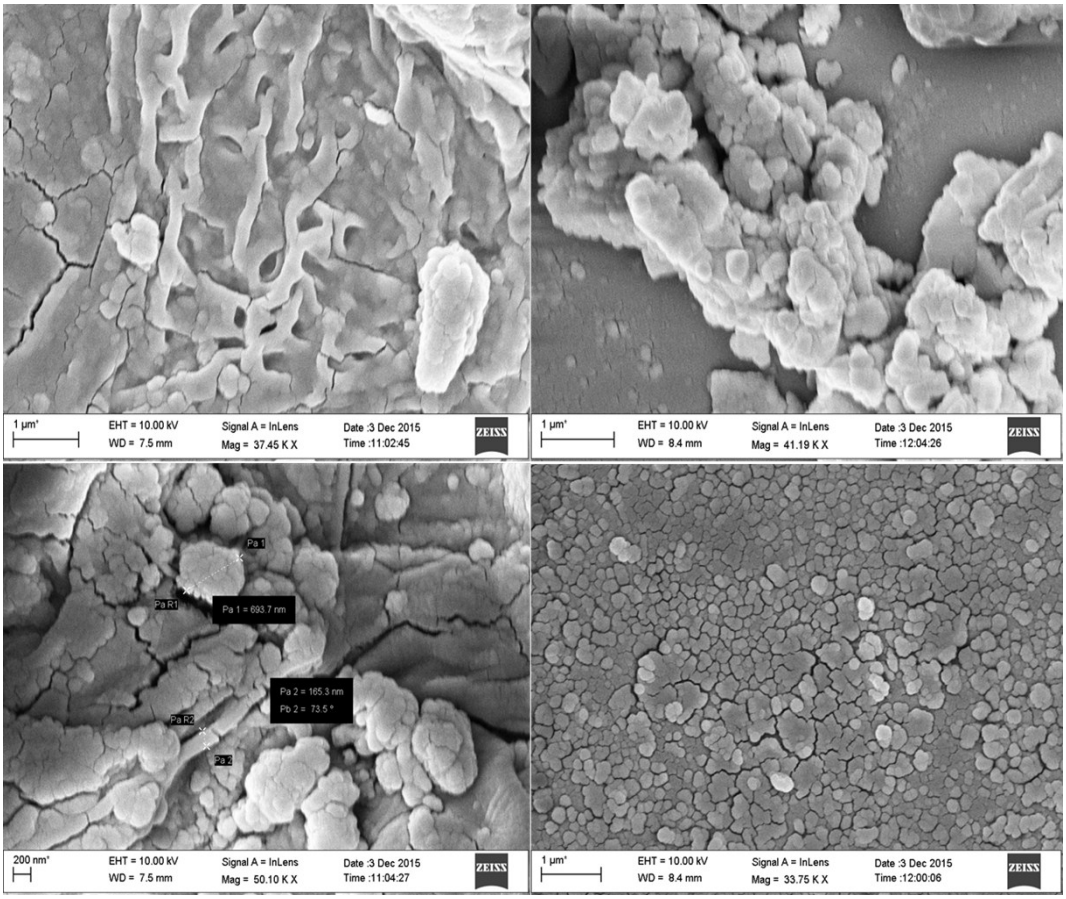

Fig. S7 Morphological changes in **PDI-DMEA** upon the addition of $Cu(ClO_4)_2$ in CH_3CN solution; Some of the Nano rods are in process of transforming into spherical structures on interaction with Cu^{2+} ions.

6. Effect of all metal ions

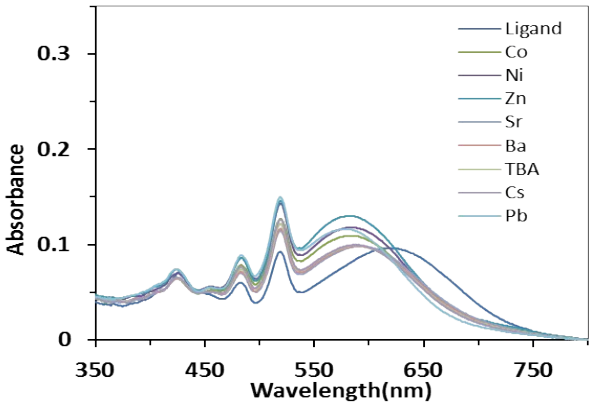

Fig. S8 Absorbance changes of **PDI-DMEA** (25 µM) in the presence of various metal ions (250 µM) recorded in CH_3CN.

7. Fluorescence data of PDI-DMEA

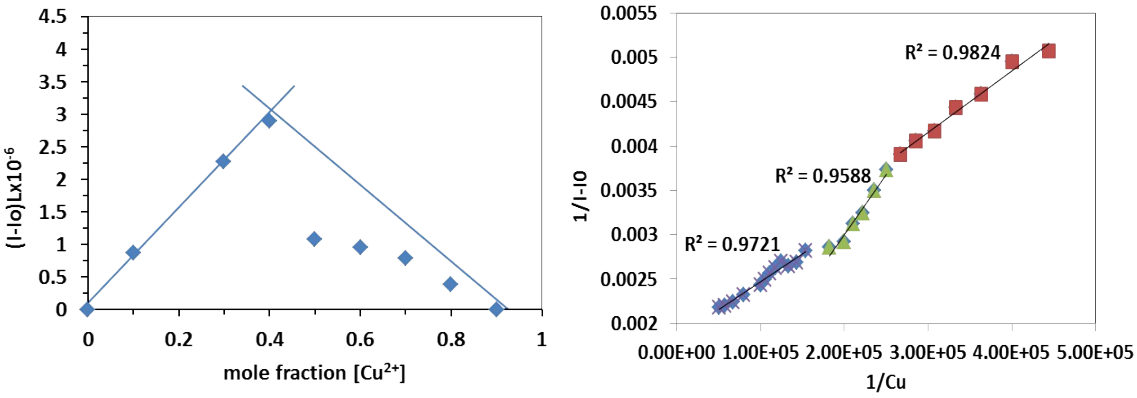

Fig. S9 (left) Job's plot (fluorimetrically) showing **PDI-DMEA**:Cu^{2+} (2:1) complex recorded CH_3CN. (right) Benesi-Hildebrand plot of **PDI-DMEA** in the presence of increasing concentrations of Cu^{2+} ions.

8. Photophysical titrations of PDI-DMEA and PDI-NH_2 with Fe^{3+}, Hg^{2+} and perchloric acid

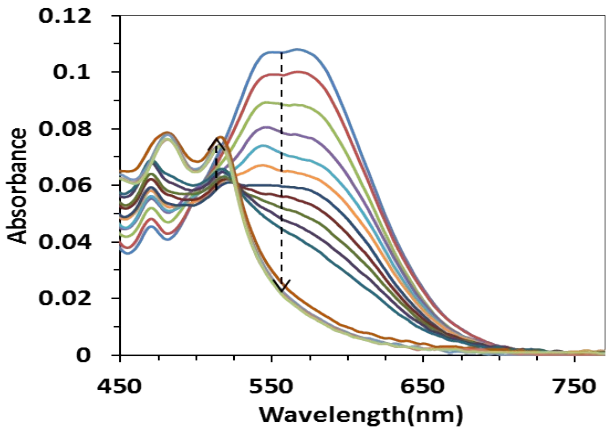

Fig. S10 UV-Vis spectra of PDI-NH_2 (25 μM) recorded in CH_3CN on addition of the Cu^{2+} ions.

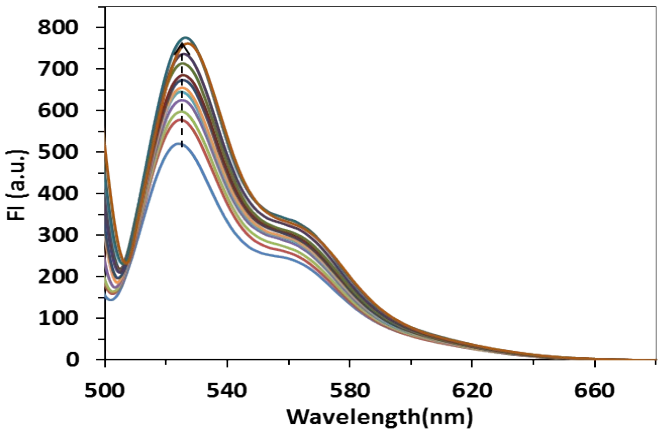

Fig. S11. Fluorescence spectra of PDI-NH_2 ($5x10^{-8}$ M) recorded in CH_3CN on addition of Cu^{2+} ions.

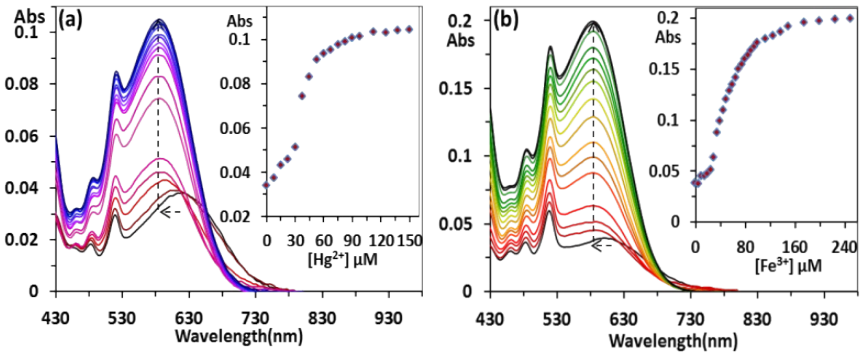

Fig. S12 UV-Vis spectra of **PDI-DMEA** (25 µM) recorded in CH_3CN on addition of (a) Hg^{2+} ions and (b) Fe^{3+} ions; Inset (a): plot of absorbance vs conc. of Hg^{2+} ions at 570 nm; Inset (b): plot of absorbance vs conc. of Fe^{3+} ions at 570 nm.

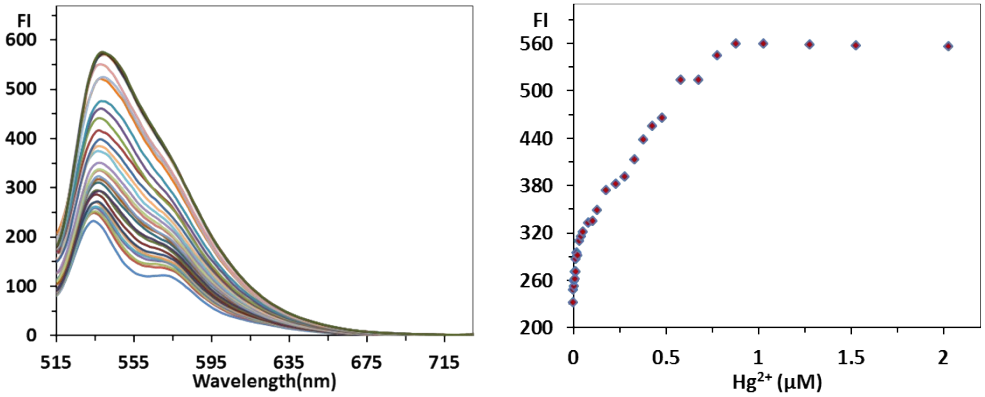

Fig. S13. Fluorescence spectra of **PDI-DMEA** ($5x10^{-8}$ M) recorded in CH_3CN on addition of Hg^{2+} ions (Left); Plot of fluorescence intensity vs conc. of Hg^{2+} ions at 530 nm (Right).

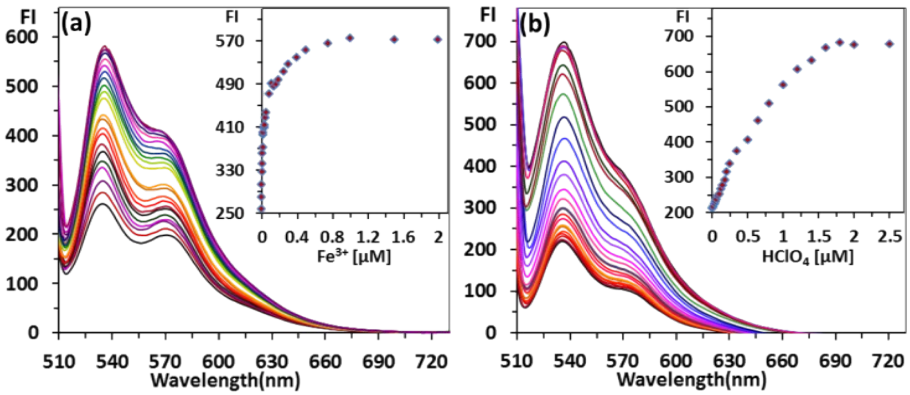

Fig. S14 Fluorescence spectra of **PDI-DMEA** ($5x10^{-8}$ M) recorded in CH_3CN on addition of (a) Fe^{3+} ions and (b) perchloric acid ($HClO_4$); Inset (a): plot of fluorescence intensity vs conc. of Fe^{3+} ions at 530 nm; Inset (b): plot of fluorescence intensity vs conc. of $HClO_4$ at 530 nm.

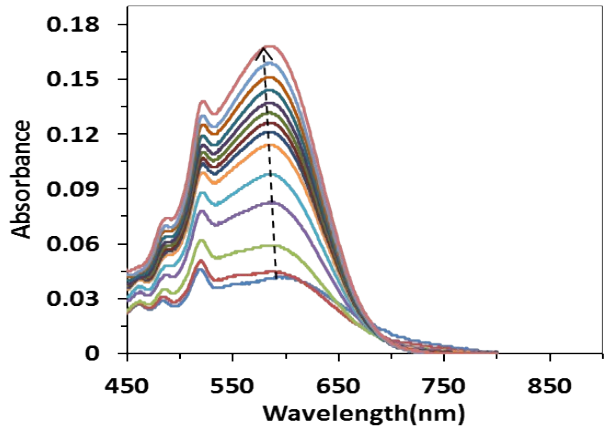

Fig. S15 Absorbance changes of **PDI-DMEA** (25 μM) on the addition of perchloric acid recorded in CH_3CN.

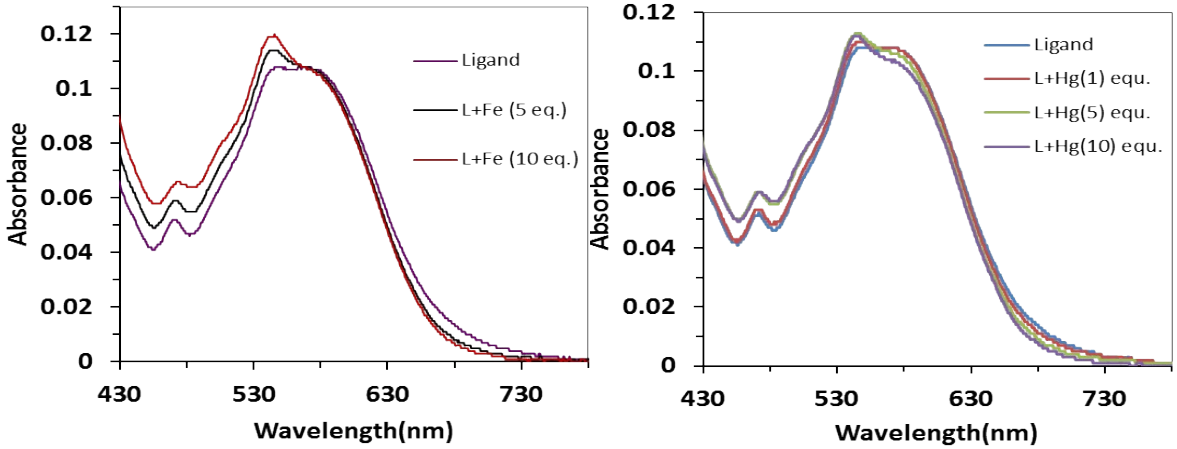

Fig. S16 UV-Vis spectra of PDI-NH_2 (25 μM) recorded in CH_3CN on addition of (a) Fe^{3+} ions and (b) Hg^{2+} ions (10 equivalent).

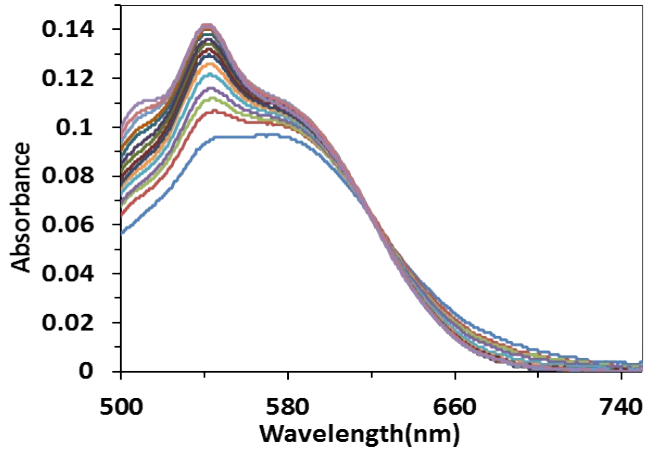

Fig. S17 Absorbance changes of PDI-NH_2 (25 μM) on the addition of perchloric acid recorded in CH_3CN.

9. Color Images of PDI-DMEA alone and in the presence of Cu^{2+} for Fluorosolvatochromism

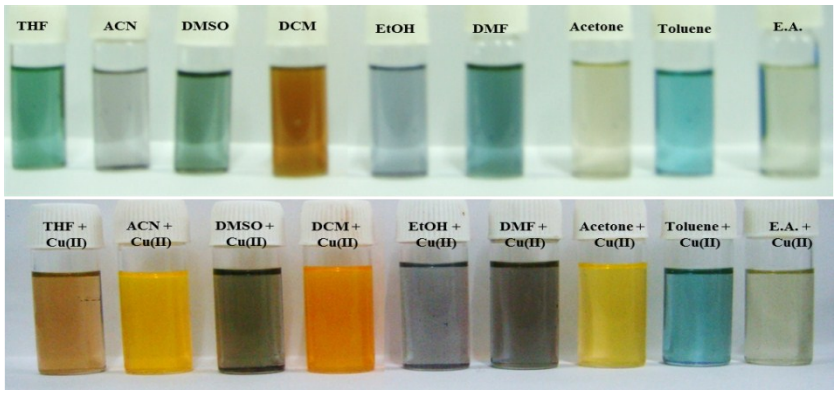

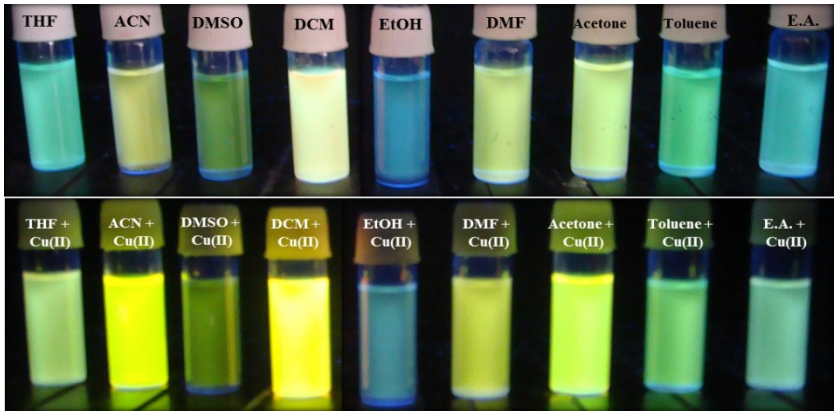

Fig. S18 PDI-DMEA can be explored for Cu^{2+} recognition in commonly used organic solvents under naked eye colour change and fluorescence colour change using hand held UV lamp, thus increasing the possibility for real application.

10. ^{1}H NMR Titration of PDI-DMEA with Cu^{2+}

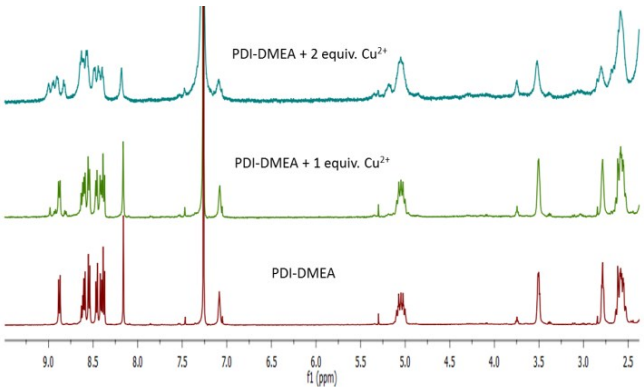

Fig. S19 Partial ^{1}H NMR spectrum of **PDI-DMEA** recorded in $CDCl_3$ upon the different additions (in equivalent) of copper perchlorate.

11. Color and fluorescent images of PDI-DMEA+Cu^{2+} complex with EDTA and CN^-

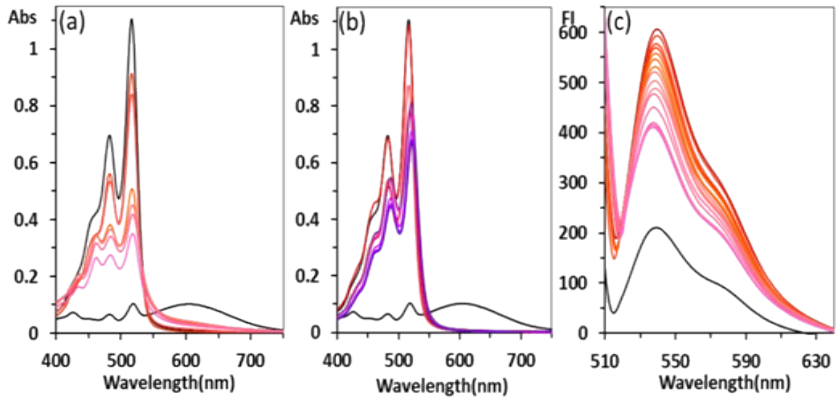

Fig. S20. (a) UV-Vis spectra of **PDI-DMEA**-Cu^{2+} (1:2) complex on addition of EDTA solution; (b) UV-Vis spectra of **PDI-DMEA**-Cu^{2+} (1:2) complex on addition of CN^- solution; (c) fluorescence spectra of **PDI-DMEA**-Cu^{2+} (1:10) complex on addition of CN^- solution; λ_{ex} = 490 nm; slit width (Ex/Em = 10/10 nm). All spectra are recorded in CH_3CN solution.

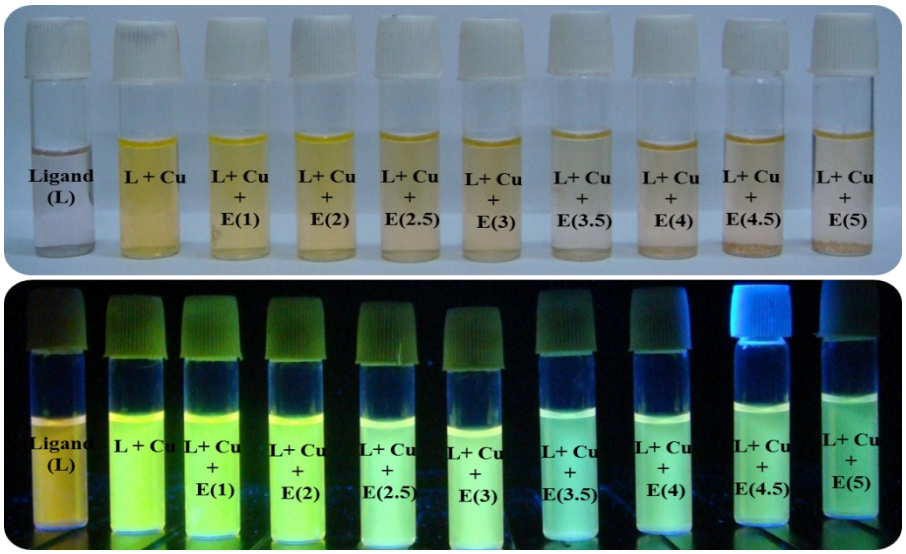

Fig. S21. Naked eye color change of **PDI-DMEA** (25 μM) and (b) Fluorescence images of **PDI-DMEA** (0.1 μM) under illumination at 365 nm UV lamp after addition of Cu^{2+} ions (50 μM) followed by addition of EDTA solution (125 μM).

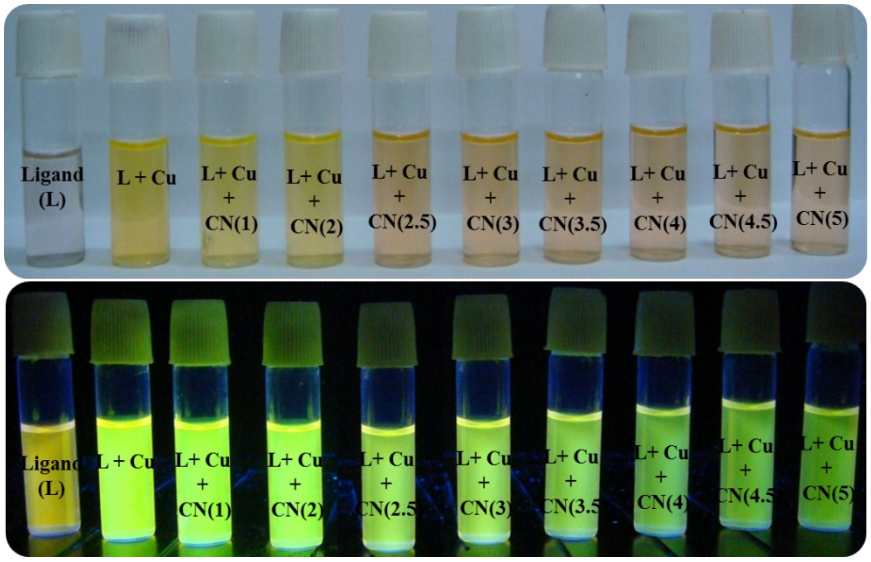

Fig. S22. Naked eye color change of **PDI-DMEA** (25 μM) and (b) Fluorescence images of **PDI-DMEA** (0.1 μM) under illumination at 365 nm UV lamp after addition of Cu^{2+} ions (50 μM) followed by addition of CN^- ions (125 μM).

12. Competition studies of Cu^{2+} in the presence of other metal ions

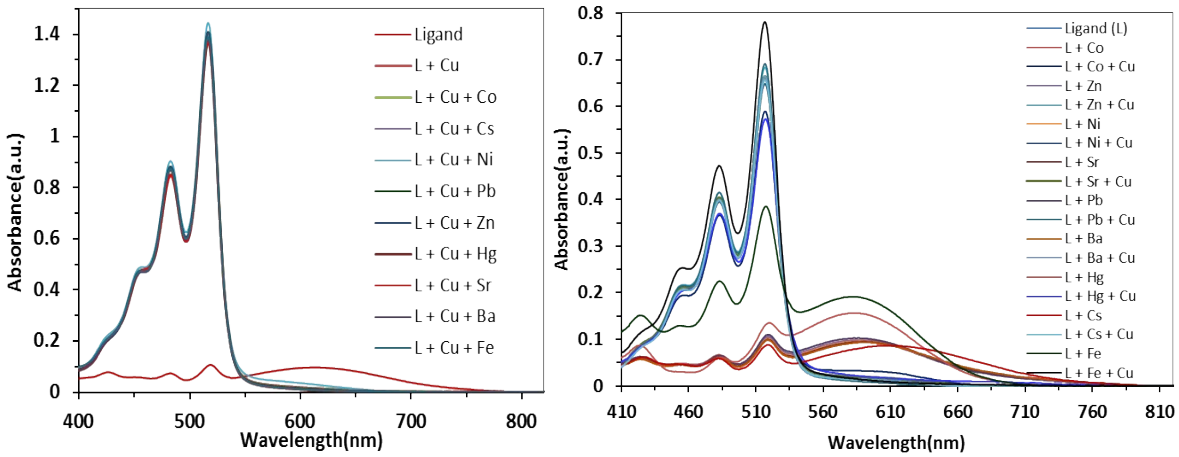

Fig. S23 The UV-Vis spectrum of **PDI-DMEA** (25 μM) in the presence of Cu^{2+} alone (50 μM) and other competitive metal ions (50 μM).